PHYSICAL REVIEW E, VOLUME 63, 010902(R)

# Entropic tempering: A method for overcoming quasiergodicity in simulation

F. Calvo*
*Departement de Recherche Fondamentale sur la Matiere Condenseé, CEA Grenoble, 17 rue des Martyrs, F38054 Grenoble Cedex, France*

J. P. K. Doye†
*University Chemical Laboratory, Lensfield Road, Cambridge CB2 1EW, United Kingdom*

(Received 30 June 2000; revised manuscript received 22 September 2000; published 20 December 2000)

The parallel tempering, multicanonical ensemble, and multiple histogram methods are combined into a powerful technique allowing enhanced sampling of complex energy surfaces. This method is shown to improve significantly the ergodic behavior in simulations of cluster melting. Application to the finite-size effects in folding minimal off-lattice $\beta$-sheet model proteins shows that the collapse and folding transitions both involve some latent heat.

DOI: 10.1103/PhysRevE.63.010902 PACS number(s): 87.15.−v, 05.10.Ln, 36.40.Ei

The ergodic hypothesis underlies the study of statistical phenomena at thermal equilibrium. However, in condensed matter physics, it is rarely discussed except in the context of glassy systems. For such systems, the time scale required for exploring all important parts of the energy landscape is much larger than the actual observation time. Finite systems can also exhibit very complex energy landscapes [1] resulting in slow dynamics and glassy behavior at low temperature. The large number of minima and high saddle points on these landscapes hinder considerably the simulation of processes such as protein folding or cluster melting. More generally, ergodic sampling of complex energy surfaces becomes harder and harder to achieve in simulation as the complexity of the interaction, the number of degrees of freedom, or the required accuracy is increased. It is also important to satisfy the ergodic hypothesis in the context of experiments in which the measurements are carried out on statistical sets or on very long time scales.

Quasiergodicity in simulation occurs when the system gets trapped into one or several basins of the energy surface, giving rise to unphysical and biased statistics and dynamics. In recent years, several authors have proposed solutions for overcoming quasiergodic behavior in simulations, as well as probes of possible nonergodicity [2]. These solutions are mostly built upon Monte Carlo (MC) methods, which are much more flexible than deterministic molecular dynamics (MD). Up to now, two main strategies have been proposed for simulating thermal equilibrium of systems having rough energy landscapes. The use of several simulations performed simultaneously and communicating with each other accelerates convergence of the low-temperature trajectories. This idea was first pioneered in the J-walking algorithm of Frantz *et al.* [3], and it was subsequently developed in the parallel versions of this algorithm [4], and in the parallel tempering method also known as the replica-exchange method [5]. Another possibility is to artificially modify the statistical probability (usually Boltzmann-like) in favor of a new distribution that is much broader in energy and less penalizing of barriers. Generalized ensembles have been built on this idea, and the corresponding simulations have used mainly either Tsallis statistics [6] or the so-called multicanonical ensemble [7]. These strategies are particularly efficient in the medium and high temperature ranges. Complementary to the problem of simulating thermal equilibrium, many ideas have been proposed to accelerate the related static problem of global optimization on complex energy landscapes.

The parallel tempering technique is very powerful and has been able to reproduce the coexisting solid phases of the 38-atom Lennard-Jones (LJ) cluster [8]. It is, however, computationally demanding, especially for this complex system where numerous and lengthy simulations have to be performed, but it is still more tractable than J-walking methods. The multicanonical ensemble, on the other hand, encounters convergence difficulties at low temperatures or energies, even when combined with simple J-walking [9]. A connection between these two methods can be made using the density of states of the system, $\Omega(E)$, which is the basic ingredient of a multicanonical simulation. This link requires an independent estimation of $\Omega$ from the parallel tempering simulation, which can be provided from a multiple histogram reweighting analysis [10]. But, even performed like this, the multicanonical simulation fails on the $LJ_{38}$ problem [8].

The inefficiency of the multicanonical ensemble sampling at low energies can be overcome using parallel tempering Monte Carlo (MC), but in a dynamical way, by adding the multicanonical MC simulation to the set of traditional MC simulations. Precisely, we assume that $m$ trajectories are performed in the canonical ensemble at the respective temperatures $\{T_i=1/k_B\beta_i\}$ where $k_B$ is the Boltzmann constant. At temperature $T_i$, the acceptance probability from configuration $\mathbf{r}_o^i$ to configuration $\mathbf{r}_n^i$ is taken as the usual Metropolis value, $\mathrm{acc}(\mathbf{r}_o^i \rightarrow \mathbf{r}_n^i)=\min(1,\exp\{-\beta_i[E(\mathbf{r}_o^i)-E(\mathbf{r}_n^i)]\})$ where $E(\mathbf{r})$ is the energy of configuration $\mathbf{r}$. We also assume that there exist a $(m+1)$th trajectory which is driven by a non-Boltzmann probability: the acceptance probability from $\mathbf{r}_o^{m+1}$ to $\mathbf{r}_n^{m+1}$ is taken as $\min[1,\exp(\{-S[E(\mathbf{r}_o^{m+1})]+S[E(\mathbf{r}_n^{m+1})]\}/k_B)]$. The entropy $S(E)$ is unknown initially, and will be determined more and more accurately during the simulation. Now, we allow occasional exchanges be-

*Electronic address: calvo@drfmc.ceng.cea.fr
†Electronic address: jon@clust.ch.cam.ac.uk

 

tween the MC trajectories. At each step, the MC moves described above are performed with a fixed probability $\chi$. With probability $1-\chi$, an exchange is attempted either between a randomly chosen trajectory $i<m$ and $j=i+1$, or between the multicanonical trajectory $j=m+1$ and the canonical trajectory $i$, which is the closest in energy at the current step. Exchanges involving the multicanonical trajectory are attempted with 50% probability. An exchange between two canonical trajectories is accepted with probability [8]

$$\mathrm{acc}(\mathbf{r}^i \rightleftharpoons \mathbf{r}^j) = \min(1, \exp\{\Delta\beta[E(\mathbf{r}^i) - E(\mathbf{r}^j)]\}), \qquad (1)$$

where $\Delta\beta = \beta_j - \beta_i$. An exchange between a canonical trajectory and the multicanonical trajectory ($j=m+1$) is accepted with probability

$$\mathrm{acc}(\mathbf{r}^i \rightleftharpoons \mathbf{r}^j) = \min\{1, \exp[\beta_i A_i(\mathbf{r}^j) - \beta_i A_i(\mathbf{r}^i)]\}. \qquad (2)$$

In this expression, we have used the Landau free energy $A_i(\mathbf{r})$ defined by $A_i(\mathbf{r}) = E(\mathbf{r}) - T_i S[E(\mathbf{r})]$. Initially, the entropy is chosen to yield a broad energy distribution, for instance by $S(E) = E/T_{\max}$ with $T_{\max}$ a ''large'' temperature, $T_{\max} > \max\{T_i\}$. After a number of steps, the simulation is interrupted and the energy histograms of the $m$ canonical trajectories are computed. A new estimate of the entropy $S = k_B \ln \Omega$ is made by least-square fitting the data to the probability $P_\beta(E)$ of observing the energy $E \pm \delta E$ at temperature $\beta$ [10]: $P_\beta(E) = \Omega(E)\exp(-\beta E)/Z(\beta)$. The multicanonical simulation proceeds with this estimate, and the entropy is regularly updated from the multiple histogram analysis of the canonical trajectories, after more and more data is added to the histograms.

This method, which we dub ''entropic tempering,'' is tested first on the $LJ_{31}$ cluster. The energy landscape of this system was recently studied by Doye, Miller, and Wales [11], who showed the existence of two low lying isomers separated by a high energy barrier. These isomers correspond to icosahedral packings with distinct surface structures, Mackay and anti-Mackay respectively. The crossover size between the two growth sequences is 31 atoms. We have simulated the finite-temperature behavior of this system using the entropic tempering method, with $m=10$ canonical simulations in the temperature range $2\times10^{-3}\varepsilon/k_B \leqslant T \leqslant 0.1\varepsilon/k_B$, ten simulations in the temperature range $0.1\varepsilon/k_B < T \leqslant 0.5\varepsilon/k_B$, and the multicanonical simulation. Since one strong advantage of the parallel tempering method is that it simultaneously acts as a global optimization algorithm, we took random geometries as starting configurations of all the MC trajectories. $1.2\times10^6$ Monte Carlo sweeps were performed for each simulation (1 sweep = 31 individual steps), and the entropy $S$ was determined after each accumulation of $10^5$ sweeps. For equilibration, the first $2\times10^5$ sweeps were discarded from the histograms. Exchanges between trajectories were attempted with the fixed probability $\chi = 10\%$. The heat capacity $C$ obtained from the final estimate of $S$ has been plotted in Fig. 1 versus the reduced canonical temperature. We have also represented the curve obtained from multicanonical MC simulations of the same length. The two curves agree well only in the melting region where the heat capacity reaches its maximum, near $T_{\mathrm{melting}} \approx 0.32$, and down to temperatures close to $0.17\ \varepsilon/k_B$ reduced units. Below this temperature, they both display an anomaly as an extra peak or bump. However, the anomalies depend on the simulation method used. In this low temperature regime, we have compared these results to calculations in the harmonic superposition approximation (HSA) [12] from the set of minima collected by Doye and co-workers [11]. The HSA prediction is ergodic by nature, because it makes no assumption about the possible pathways between the isomers. Even though it would require a very large set of stationary points to extend its range of validity up to the melting region, it shows that the coexistence of the two low-energy minima induces a narrow phase change at about $T \sim 0.03\varepsilon/k_B$. Only the entropic tempering calculation is able to reproduce this transition quantitatively. Pure multicanonical sampling does not converge at low temperatures, and displays variations of the caloric curve below $0.17\varepsilon/k_B$ that cannot be reproduced. A more difficult example is the 38-atom LJ cluster, because of its double-funnel energy landscape [13]. We have been able to obtain results in agreement with the work of Neirotti *et al.* [8] with only 30 simulations of $3\times10^8$ steps each, compared to $1.3\times10^{10}$ in the original work. Another good test, but even harder than $LJ_{38}$, would be the decahedral 75-atom LJ cluster.

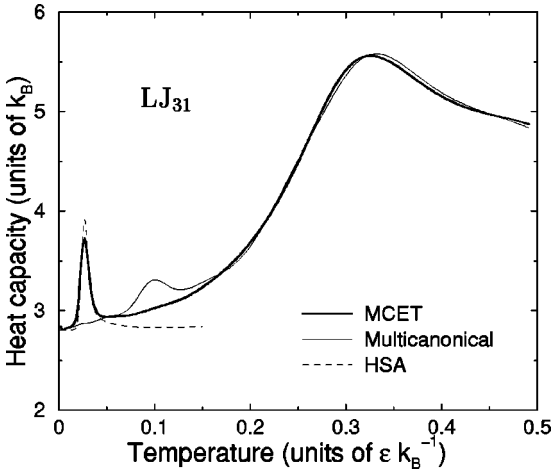


FIG. 1. Heat capacity per atom of the 31-atom Lennard-Jones cluster vs the canonical temperature, per unit of $k_B$. The results of Monte Carlo entropic tempering (MCET, thick solid line), multicanonical MC (thin solid line), and superposition approximation (HSA, dashed line) are represented.

As a further application of the entropic tempering method, we have investigated finite-size effects in the thermodynamics of a model protein. Many authors have characterized the folding thermodynamics of lattice and off-lattice models by considering the variations of the heat capacity versus temperature [14]. In the present work, we have chosen a simple off-lattice model developed by Honeycutt and Thirumalai [15], which predicts native states of the $\beta$-sheet form. This three-letter model, often called the ''BLN'' model, has been widely studied by a variety of groups, with some minor changes in the parameters [16–20]. In particular, for the 46-

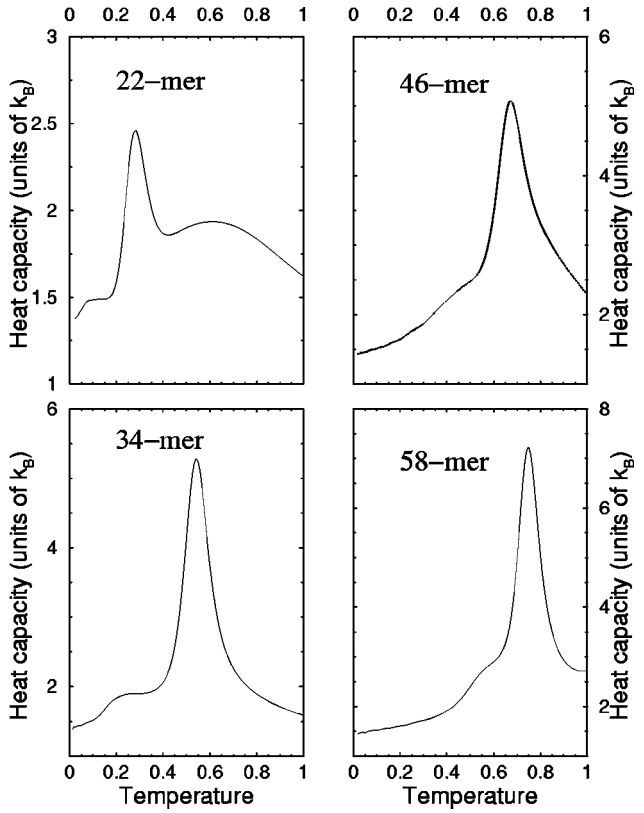


FIG. 2. Heat capacities per residue of four $\beta$-sheet model proteins, in units of $k_B$ for $N=22$ (two sheets), 34 (three sheets), 46 (four sheets), and 58 (five sheets).

mer sequence (four sheets), the energy landscape [17], thermodynamics [15,18], and kinetics [19] have been characterized. It has also been used as a benchmark for global optimization [20]. More generally, this model displays rough energy landscapes that cannot be sampled by conventional simulation methods. We use here the same values of the parameters as Berne and co-workers [20], including the nonrigid bond lengths between successive residues. Four sequences have been considered, containing 2, 3, 4, and 5 $\beta$ strands or 22, 34, 46, and 58 residues, respectively [21]. Thirty MC simulations at reduced temperatures in the range $10^{-2} \leqslant T \leqslant 1.5$ were performed during $10^6$ sweeps following $2\times10^5$ equilibration sweeps, and again with 10% probability for attempting an exchange. The heat capacities for the four model proteins are shown in Fig. 2. All curves show a clear peak which is characteristic of a transition from coil states to a set of collapsed states, but not only consisting of the native state [19]. This transition can also be observed in the variations of the radius of gyration (not plotted here). Another interesting feature of the caloric curves is that they also display an anomaly at temperatures lower than the collapse temperatures defined as the heat capacity maxima. The shoulder in the heat capacity is particularly marked for the two-, three-, and five-strand systems. In the case of the four-strand protein, our results are in agreement with those obtained by Guo and Brooks [18] (within the small differences in the models used), but qualitatively different from those of Nymeyer *et al.* [22]. Following previous investigations of this

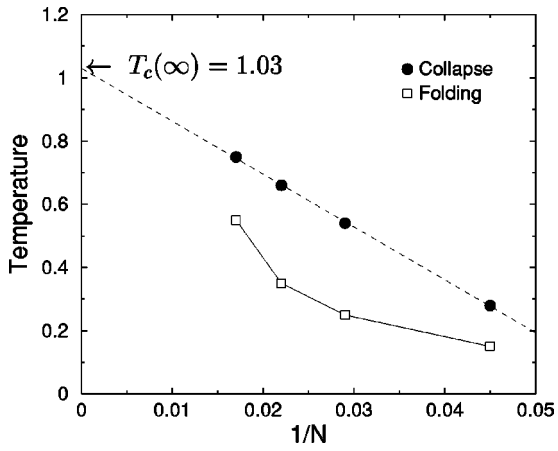


FIG. 3. Variations of the collapse (closed circles) and folding (open squares) temperatures of the BLN heteropolymers vs $1/N$. The straight dashed line is the extrapolation to large numbers of strands.

system [18], the thermal anomalies can be interpreted as signatures of the transition from the collapsed states to the native state, that is the true folding transition. Some support for this interpretation can be provided by the calculation of the temperature dependence of the structural overlap with the native state [18]. Since many (but not all) model proteins show such a behavior, it seems important to note that the multiple-step folding of this model system is very similar to the multiple-step melting of many atomic clusters [23].

Because of the presence of anomalies in the heat capacities, it is difficult to extract the critical exponents of finite-size scaling theory for this system [24]. However, by analogy to the recent analysis of the helix-coil transition by Hansmann and co-workers [24], we assume that the present model proteins can be considered as one-dimensional objects. We also assume that the collapse transition is a first-order one [24]. Defining the folding temperature $T_f$ by the occurrences of the anomalies, we can evaluate the variations of both $T_c$ and $T_f$ versus $1/N^\alpha$, with $\alpha \approx 1$ represented in Fig. 3. Two interesting features can be observed. First, the folding temperature becomes closer to the collapse temperature as size increases. This is similar to what is observed in clusters [23], and we will assume that it holds for proteins much larger than those presently investigated. Also, the fit to a straight line for $T_c(1/N)$ is very good. Using the previous assumption, it allows us to estimate the folding temperature for proteins having a large number of $\beta$ strands: $T_f(N\rightarrow\infty) \approx T_c(N\rightarrow\infty) \approx 1.03$ reduced units.

The present results show that the heteropolymer ''BLN'' model generally exhibits multistep folding in a range of sizes. It would be valuable to know how this phenomenon evolves when the number of strands increases (e.g., to check the previous prediction), and when the length of the strands increases. In particular, a relative decrease of the heat capacity anomaly with respect to the main collapse peak would be another similarity with cluster melting [23]. Other size effects resulting from more complex (i.e., not all-$\beta$) native states could also be investigated.

The entropic tempering technique incorporates the calcu-

lation of the microcanonical entropy $S$ as a function of the energy. This function contains much more information than the microcanonical caloric quantities. In addition to the canonical properties obtained by Laplace transformation, the density of states can be used in other situations, for example, to calculate statistical rates of evaporation or fragmentation [25], or to classify the order of a transition from the zeros of the partition function in the complex plane [24,26]. The parallel tempering exchanges are the key ingredient for accelerating convergence and ensuring ergodicity at low temperature. By combining this method with multicanonical sampling, the entropic tempering scheme allows fewer and shorter simulations to be used, and at the same time provides a reliable estimate of the density of states. The density of states, in turn, is the fundamental element of all thermodynamical functions.

In the present work, the entropic tempering method was described in the framework of the canonical ensemble. By changing the Boltzmann exponential weights in the acceptance probabilities, it is possible to improve further the sampling efficiency by using Tsallis polynomial weights, or several multicanonical trajectories. The microcanonical and molecular dynamics (MD) ensemble (with additional constraints on the total linear and angular momenta) can also be sampled by taking the appropriate weights. A further coupling with standard MD simulations into a hybrid MC-MD algorithm will then provide a way for molecular dynamics to become ergodic. With these various possible enhancements and the ease of its implementation, we believe that entropic tempering is an efficient, general-purpose strategy for reducing the quasiergodic behavior in simulation of complex systems.

*Note added in proof.* After this article was accepted for publication, we found another work using different combinations of the multicanonical and parallel tempering methods [Chem. Phys. Lett. **329**, 261 (2000)], which, however, do not seem to be far superior to the multicanonical sampling alone at low temperatures.

One of us (F.C.) wishes to thank Professor D. L. Freeman and Professor P. Labastie for useful discussions.

[1] D. J. Wales, M. A. Miller, and T. R. Walsh, Nature (London) **394**, 758 (1998).
[2] R. D. Mountain and D. Thirumalai, Physica A **210**, 453 (1994).
[3] D. D. Frantz, D. L. Freeman, and J. D. Doll, J. Chem. Phys. **93**, 2769 (1990).
[4] A. Matro, D. L. Freeman, and R. Q. Topper, J. Chem. Phys. **104**, 8690 (1996); A. Dullweber, M. P. Hodges, and D. J. Wales, *ibid.* **106**, 1530 (1997).
[5] E. Marinari and G. Parisi, Europhys. Lett. **19**, 451 (1992).
[6] I. Andricioaei and J. E. Straub, J. Chem. Phys. **107**, 9117 (1997); U. E. Hansmann and Y. Okamoto, Phys. Rev. E **56**, 2228 (1997).
[7] B. A. Berg and T. Neuhaus, Phys. Rev. Lett. **68**, 9 (1991).
[8] J. P. Neirotti *et al.*, J. Chem. Phys. **112**, 10 340 (2000).
[9] H. Xu and B. J. Berne, J. Chem. Phys. **110**, 10 299 (1999).
[10] A. M. Ferrenberg and R. H. Swendsen, Phys. Rev. Lett. **61**, 2635 (1988); P. Labastie and R. L. Whetten, *ibid.* **65**, 1567 (1990).
[11] J. P. K. Doye, M. A. Miller, and D. J. Wales, J. Chem. Phys. **111**, 8417 (1999).
[12] D. J. Wales, Mol. Phys. **78**, 151 (1993).
[13] J. P. K. Doye, M. A. Miller, and D. J. Wales, J. Chem. Phys. **110**, 6896 (1999).
[14] See, for instance, N. D. Socci and J. N. Onuchic, J. Chem. Phys. **103**, 4732 (1995).
[15] J. D. Honeycutt and D. Thirumalai, Biopolymers **32**, 695 (1992).
[16] R. S. Berry *et al.*, Proc. Natl. Acad. Sci. U.S.A. **94**, 9520 (1997); B. Vekhter and R. S. Berry, J. Chem. Phys. **110**, 2195 (1998).
[17] M. A. Miller and D. J. Wales, J. Chem. Phys. **111**, 6610 (1999).
[18] Z. Guo and C. L. Brooks, III, Biopolymers **42**, 745 (1997).
[19] Z. Guo and D. Thirumalai, Biopolymers **36**, 83 (1995).
[20] P. Amara and J. E. Straub, J. Phys. Chem. **99**, 14840 (1995); Y.-H. Lee and B. J. Berne, J. Phys. Chem. A **104**, 86 (2000).
[21] The detailed sequences for the two-, four-, and five-sheet proteins can be found in Refs. [15] and [20]. For the three-sheet system, the sequence is $L(BL)_4N_3B_9N_3(BL)_5$.
[22] H. Nymeyer, A. E. García, and J. N. Onuchic, Proc. Natl. Acad. Sci. U.S.A. **95**, 5921 (1998).
[23] F. Calvo and F. Spiegelmann, Phys. Rev. Lett. **82**, 2270 (1999).
[24] N. A. Alves and U. H. E. Hansmann, Phys. Rev. Lett. **84**, 1836 (2000); J. Kemp, U. H. E. Hansmann, and Z. Y. Chen, Eur. Phys. J. B **15**, 371 (2000).
[25] S. Weerasinghe and F. G. Amar, J. Chem. Phys. **98**, 4967 (1993).
[26] P. Borrmann, O. Mulken, and J. Harting, Phys. Rev. Lett. **84**, 3511 (2000).